ChemComm

Accepted Manuscript

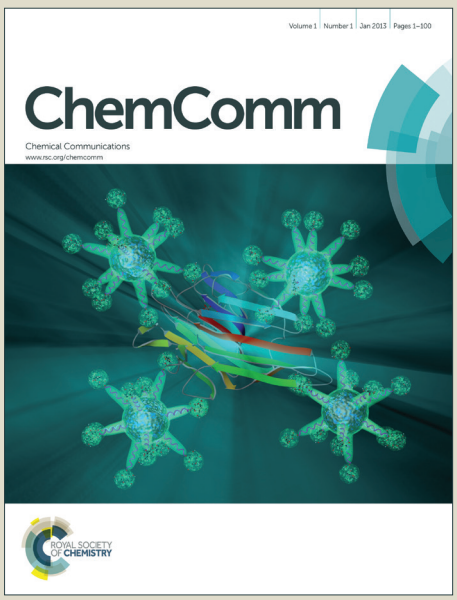

ROYAL SOCIETY OF CHEMISTRY

www.rsc.org/chemcomm

Chemical Communications ChemComm

Cite this: DOI: 10.1039/c0xx00000x

www.rsc.org/xxxxxx

Communication

Fluorescent hydrogels for studying Ca^{2+}-dependent reaction-diffusion processes

Sergey N. Semenov,[a] Sjoerd G.J. Postma,[a] Ilia N. Vialshin,[a] and Wilhelm T.S. Huck[a]

Received (in XXX, XXX) Xth XXXXXXXXX 20XX, Accepted Xth XXXXXXXXX 20XX
DOI: 10.1039/b000000x

Here, we report a convenient experimental platform to study the diffusion of Ca^{2+} in the presence of a Ca^{2+}-binding protein (Calbindin D28k). This work opens up new methods to elucidate the physical chemistry of complex Ca^{2+}-dependent reaction-diffusion networks that are abundant in living cells.

Ca^{2+} is a pivotal second messenger involved in a wide variety of complex cellular networks.[1,2] Reaction-diffusion (RD) processes where interactions between molecules take place at similar timescales as their diffusion,[3,4] play an essential role in Ca^{2+} signalling.[1,5] In the highly crowded cytosol, Ca^{2+} diffusion profiles are influenced by both fixed and mobile Ca^{2+}–binding proteins, and non-specific interactions with other proteins and charged surfaces.[6] Although the advent of organic Ca^{2+} sensors has enabled studies on Ca^{2+} dynamics *in vivo*,[7] the determination of individual contributions of Ca^{2+}-binding proteins and other factors to RD networks requires an artificial platform that avoids cellular complexity. Previous efforts using $^{45}Ca^{2+}$ could only measure the total amount of Ca^{2+} in a sample, and thin slices of a frozen gel needed to be analysed, thus precluding continuous measurements of Ca^{2+} diffusion.[5,8] In a different approach, Ca^{2+} sensors which diffused through a gel were applied.[9–11] However, this method results in a system in which not only Ca^{2+}, but also the indicator and the Ca^{2+}-indicator complex diffuse, thereby complicating the equations used to describe the RD processes. Here, we present hydrogels with a covalently linked fluorescent Ca^{2+}-indicator. Our approach prevents diffusion of the indicator whilst taking advantage of facile probing of Ca^{2+} diffusion in time by fluorescence microscopy. By applying a wet stamping technique,[12,13] we show that the influence of a Ca^{2+}-binding protein on Ca^{2+} diffusion can be monitored and modelled, taking the first steps towards building complex Ca^{2+}-dependent RD networks *in vitro*.

We chose 10 wt% polyacrylamide (PAAm) and 9 wt% polyethylene glycol (PEG) cross-linked hydrogels as polymer matrices for our materials, since they are readily prepared and require little modification of a Ca^{2+}-sensing dye. The Ca^{2+} sensor Indo-1 was chosen for the fluorescent read-out. Indo-1 is an ideal sensing element, as a derivative of this Ca^{2+} indicator has already been successfully coupled to polymeric beads,[14] and it displays an emission shift upon Ca^{2+} binding,[15] allowing facile visualization of the diffusion front.

In order to covalently attach Indo-1 to a hydrogel matrix we attached linker moieties to the carboxyl group of the indole ring (Scheme 1),[14,16] as this site is not involved in the chelating properties of the 1,2-bis(2-aminophenoxy)ethane-N,N,N',N'-tetraacetic acid (BAPTA) fragment. We obtained 5-[6-carboxy-indol-2-yl]-5'-methyl-BAPTA ethyl ester following the protocols of Bradley *et al.*[14] Subsequent experiments showed that the indole carboxyl group can be activated *via* the formation of an *N*-hydroxysuccinimide (NHS) ester (**1**). Gratifyingly, compound **1** was sufficiently stable to be purified by column chromatography. Activation of carboxylic acids by NHS ester formation is widely used for attachment of target molecules to surfaces and proteins *via* free amines. Compound **1** is therefore a useful addition to the toolbox of NHS-functionalized fluorophores.

Reactions of **1** with two different amines yielded Indo-1 derivatives with either a methylacrylamide ($IndoL_1$) or alkene

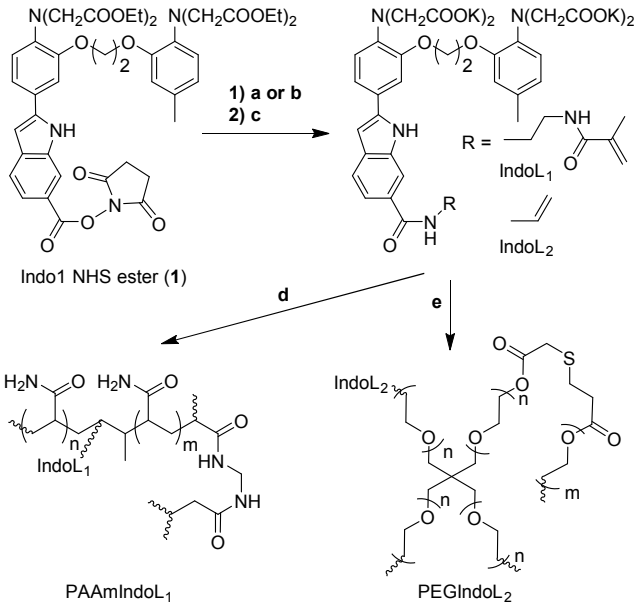

Scheme 1 Synthesis of Indo-1-based Ca^{2+}-sensing gels. a) (3-aminopropyl)methacrylamide hydrochloride, DIPEA, DMF (solv.), 2.5 h, r.t., 13% b) allylamine, DMF (solv.), 2.5 h, r.t., 50% c) KOH, THF:MeOH (4:1, v/v), o.n., r.t., 65% d) $IndoL_1$, acrylamide, bisacrylamide, $CaCl_2$, 2,2'-azobis(2-methyl-propionamidine) dihydrochloride (AAPH), UV (λ_{ex} = 365 nm) e) $IndoL_2$, bis-acryl-PEG-10000, Thio-4ArmPEG-2000, $CaCl_2$, lithium arylphosphonate (LAP), UV (λ_{ex} = 365 nm)

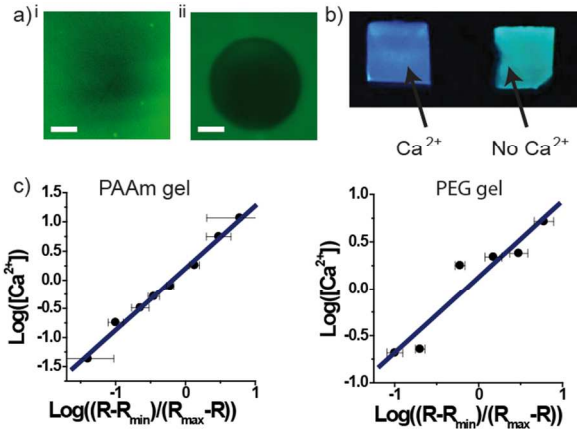

Fig. 1 Characterization of hydrogels. (a) False-colour images of the FRAP experiment for the PAAmIndoL$_1$ gel. (i) Gel with diffusing IndoL$_1$ 10 minutes after bleaching. (ii) Gel with co-polymerized IndoL$_1$ two days after bleaching. Scale bars are 500 µm. (b) Real-colour photo of PAAmIndoL$_1$ gel with and without Ca^{2+}. (c) Calibration curves for PAAmIndoL$_1$ and PEGIndoL$_2$ gels. R is the ratio of emission intensity at 405 nm *vs* 520 nm. R_{min} and R_{max} are the ratio's for fully unsaturated and saturated indicator, respectively.

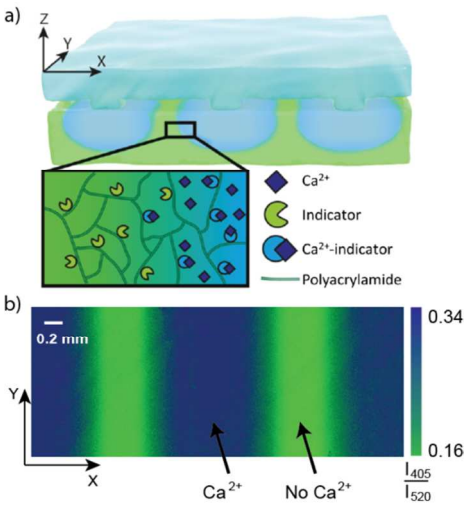

Fig. 2 (a) Schematic representation of the experimental setup. A Ca^{2+}-soaked agarose stamp with pillars is placed on top of an PAAmIndoL$_1$ gel. (b) A typical I_{405}/I_{520} image obtained by dividing two images of a Ca^{2+} diffusion experiment taken with different emission wavelength filters. The gel was imaged from below.

(IndoL$_2$) functionality. Both derivatives show a blue shift of the emission spectrum upon Ca^{2+} binding. Dissociation constants (K_d) for IndoL$_1$ and IndoL$_2$ were determined to be 514 and 340 nM, respectively, and the selectivity of IndoL$_1$ towards Ca^{2+} was demonstrated (see ESI). Next, both sensor molecules were incorporated into hydrogels *via* co-polymerization. We prepared the hydrogels by photoinitiation in the presence of indicator-saturating concentrations of Ca^{2+} to reduce decomposition of the fluorophore.[17]After initial washings, we placed the gel in a solution with a BAPTA-functionalized PAAm gel (see ESI). In this way, we removed residual amounts of Ca^{2+} while avoiding the use of diffusing Ca^{2+} chelators that would complicate RD experiments.

To prove that the Ca^{2+} sensor was covalently attached to the PAAm gel, a fluorescence recovery after photobleaching (FRAP) experiment was performed (Fig 1a). We compared two samples: (i) PAAm hydrogel doped with 10 µM free IndoL$_1$ solution after polymerization, and (ii) PAAm hydrogel with 10 µM co-polymerized IndoL$_1$. The fluorescence in the bleached region was restored within 10 minutes in the first sample, while the second sample did not show any recovery after two days.

The response of the PAAmIndoL$_1$ gel towards Ca^{2+} was visible by the naked eye (Fig. 1b) and reversible (see ESI). To perform quantitative characterization of the gel response, pieces of PAAmIndoL$_1$ and PEGIndoL$_2$ gel were equilibrated with buffers containing 0 to 39 µM of free Ca^{2+}. The gels were then imaged by fluorescence microscopy (λ_{ex} = 365 nm, λ_{em} = 405 or 520 nm). Figure 1c depicts the calibration curves obtained in this way. A detection range from 0.1 to 3 µM Ca^{2+} for PAAmIndoL$_1$ could be assumed from the plot. The K_d of 490 nM calculated for PAAmIndoL$_1$ from this curve was in good agreement with our data for IndoL$_1$ in solution, showing that copolymerization did not lead to changes in the Ca^{2+}-sensing properties of IndoL$_1$.

The calibration curves showed that the PEGIndoL$_2$ gel has a similar detection range for Ca^{2+} as PAAmIndoL$_1$, but the latter is more accurate. Moreover, whereas the PAAmIndoL$_1$ gel swelled by 18% its initial volume during washings, for the PEGIndoL$_2$ gel this value was 400%. Therefore, the PEGIndoL$_2$ hydrogel is suitable for applications requiring soft 3D gels, but is less convenient for accurate determination of Ca^{2+} concentrations. For that reason, we chose to use the PAAmIndoL$_1$ gel in further experiments.

We demonstrate the application of the PAAmIndoL$_1$ gel for quantitative studies on RD of Ca^{2+} in a wet stamping experiment depicted in Fig. 2a.[12,13] The great advantage of this method is that the initial conditions (*i.e.* starting time, points of contact, and concentrations) are well-defined. A 6 wt% agarose stamp with an array of parallel lines (500 µm wide, 200 µm high and spaced by 1500 µm) was soaked in a $CaCl_2$ solution for at least 15 hours, and placed feature-side-down on top of a piece of PAAm-IndoL$_1$ gel (0.4 mm high). Next, a series of fluorescence images was acquired. At every 30 seconds time point, ratios of intensities at 405 and 520 nm (I_{405}/I_{520}) were determined by dividing two images that were taken at these different emission wavelengths within 1 second of each other (Fig. 2b).

In the first series of experiments we varied the initial concentration of free Ca^{2+} in the stamp. As one should expect, we observed an increase in the rate of propagation of the diffusion front with higher initial concentrations of Ca^{2+} (Fig. 3a). I_{405}/I_{520} values were converted to a profile of Ca^{2+} concentrations by using a calibration curve (Fig. 3b). This transformation is valid if we assume a flat diffusion front (pseudo-1D diffusion).

Next, we demonstrate the potential of our platform for *in vitro* studies on Ca^{2+}-dependent RD processes by carrying out an experiment involving Calbindin-D28k (CalB). CalB is a protein abundant in neurons, and is able to bind up to four Ca^{2+} ions.[18] We soaked the PAAmIndoL$_1$ gel in a buffer containing CalB (30 µM final concentration), and stamped it with an agarose gel equilibrated in a buffer with 25 µM $CaCl_2$. Time-space plots allowed visualization of the diffusion process (Fig. 4a). Compared to analogous experiments in the absence of Ca^{2+}-binding protein, we clearly observed slower propagation of the Ca^{2+} diffusion front when CalB was present. Because of the slow diffusion, the front is not flat and a model of 2D diffusion is

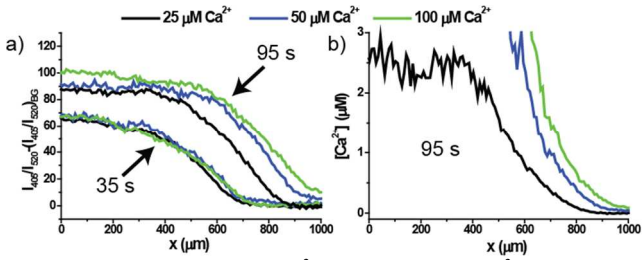

Fig. 3 Influence of the initial Ca^{2+} concentration on Ca^{2+} diffusion. (a) Change of diffusion profiles in time for experiments with different Ca^{2+} concentrations in the stamp. (b) Calculated [Ca^{2+}] profiles for the 95 second time point assuming a flat diffusion front. Considering the sensitivity of our gel, 3 μM Ca^{2+} is the upper detection limit.

required.[12,13] The inherent control of the wet stamping technique allowed us to simulate the RD experiment using COMSOL (Fig. 4b and ESI). A symmetry-independent element of the experimental setup was constructed to model reaction-diffusion through a half-pillar of the agarose stamp on top of the PAAmIndoL$_1$ gel (Figure 4b). As the stamp used in the RD experiment is much thicker than the pillar and the PAAmIndoL$_1$ gel, we maintained the Ca^{2+} concentration at the top of the stamp at 25 μM (grey line in Fig. 4b) assuming a continuous source of Ca^{2+}. The reactions included in the simulation are the four reversible binding events of Ca^{2+} to CalB (30 μM) and one for Ca^{2+} binding to IndoL$_1$. Ca^{2+}, CalB and the four Ca^{2+}-CalB complexes were the only species allowed to diffuse. As can be seen in Figure 4c, there is an excellent fit between model and experimental data, especially at the early time points. In addition to the concentration of free Ca^{2+} depicted in Fig. 4b, all other components (Ca^{2+}-bound or -free IndoL$_1$ and CalB) could be profiled in the model as well (see ESI).

In conclusion, we demonstrated that our PAAmIndoL$_1$ hydrogel can be applied to quantitatively monitor Ca^{2+} diffusion in the presence of a Ca^{2+}-binding protein. The wet stamping method is ideally suited to determine binding constants between diffusing and immobile species.[12] The change in steepness of the Ca^{2+}-diffusion front in the presence of CalB is an indication that we can study ultrasensitivity and molecular titration effects.[13] In future experiments, mobile and stationary Ca^{2+} buffers, the influence of dimensionality, and photo-initiated release of caged Ca^{2+} to mimic intracellular Ca^{2+} signals can be studied with our platform. Moreover, we can exploit the reversible binding of Ca^{2+} to the sensor hydrogel to investigate pattern formation in complex Ca^{2+}-dependent RD networks in order to increase our understanding of RD processes and cellular complexity.

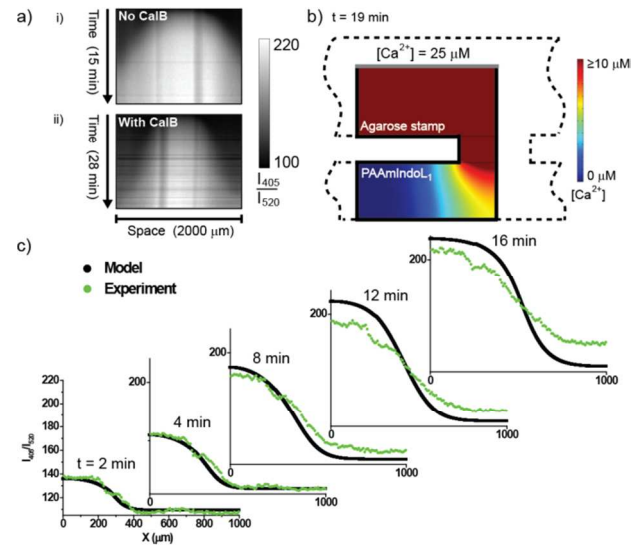

Fig. 4 Experimental data and modelling of RD of Ca^{2+} (25 μM in the stamp) in the presence of Calbindin D28K (CalB, 30 μM). (a) Time-space plots of Ca^{2+} RD with a pillar of the stamp at the center of the image in (i) the absence and (ii) the presence of CalB. (b) Computer model of the RD experiment 19 minutes after its start. The concentration of free Ca^{2+} is depicted. The solid black border denotes that no flux is possible at those points, and the gray border that the Ca^{2+} concentration is constant. (c) Comparison of Ca^{2+} diffusion profiles of the RD experiment (green lines) to the simulations (black lines) at different time points.

We thank Dr. Wim Scheenen for fruitful discussions. We acknowledge financial support from the European Research Council (ERC; Advanced Grant 246812 Intercom), the Netherlands Organisation for Scientific Research (NWO,VICI Grant 700.10.44 (W.T.S.H.) a Marie Curie Intra-European Fellowship (Grant 300519 to S.N.S.) and funding from the Ministry of Education, Culture and Science (Gravity program 024.001.035).

Notes and references

[a] *Institute for Molecules and Materials, Radboud University Nijmegen, Toernooiveld 1, 6525 ED, Nijmegen, The Netherlands. E-mail: w.huck@science.ru.nl, Tel.: +31 (0)24 3652138 Fax: +31 (0) 243652929.*

† Electronic Supplementary Information (ESI) available: including details of the synthesis of Indo-1 and BAPTA derivatives, gel preparation and properties, RD experiments, and modelling. See DOI: 10.1039/b000000x/

1. M. J. Berridge, M. D. Bootman, and H. L. Roderick, *Nat. Rev. Mol. Cell Biol.*, 2003, **4**, 517–529.
2. M. J. Berridge, P. Lipp, and M. D. Bootman, *Nat. Rev. Mol. Cell. Biol.*, 2000, **1**, 12–21.
3. S. Soh, M. Byrska, K. Kandere-Grzybowska, and Bartosz A. Grzybowski, *Angew. Chem. Int. Ed.*, 2010, **49**, 4170–4198.
4. S. Kondo and T. Miura, *Science*, 2010, **329**, 1616–1620.
5. N. L. Allbritton, T. Meyer, and L. Stryer, *Science*, 1992, **258**, 1812–1815.
6. D. E. Clapham, *Cell*, 2007, **131**, 1047–1058.
7. C. Grienberger and A. Konnerth, *Neuron*, 2012, **73**, 862–885.
8. J. J. Feher, C. S. Fullmer, and G. K. Fritzsch, *Cell Calcium*, 1989, **10**, 189–203.
9. M. H. Wussling, K. Krannich, V. Drygalla, and H. Podhaisky, *Biophys. J.*, 2001, **80**, 2658–2666.
10. M. H. P. Wussling, I. Aurich, O. Knauf, H. Podhaisky, and H.-J. Holzhausen, *Biophys. J.*, 2004, **87**, 4333–4342.
11. M. H. Wussling, K. Krannich, G. Landgraf, A. Herrmann-Frank, D. Wiedenmann, F. N. Gellerich, and H. Podhaisky, *FEBS Lett.*, 1999, **463**, 103–109.
12. Y. Wei, P. J. Wesson, I. Kourkine, and B. A. Grzybowski, *Anal. Chem.*, 2010, **82**, 8780–8784.
13. S. N. Semenov, A. J. Markvoort, W. B. L. Gevers, A. Piruska, T. F. A. de Greef, and W. T. S. Huck, *Biophys. J.*, 2013, **105**, 1057–1066.
14. R. M. Sánchez-Martín, M. Cuttle, S. Mittoo, and M. Bradley, *Angew. Chem. Int. Ed. Engl.*, 2006, **45**, 5472–5474.
15. G. Grynkiewicz, M. Poenie, and R. Y. Tsien, *J. Biol. Chem.*, 1985, **260**, 3440–3450.
16. M. Bannwarth, I. R. Correa, M. Sztretye, S. Pouvreau, C. Fellay, A. Aebischer, L. Royer, E. Rois, and K. Johnsson, *ACS Chem. Biol.*, 2009, **4**, 179–190.
17. W. J. J. M. Scheenen, L. R. Makings, L. R. Gross, T. Pozzan, and R. Y. Tsien, *Chem. & Biol.*, 1996, **3**, 765–774.
18. K. G. Baimbridge, M. R. Celio, and J. H. Rogers, *Trends Neurosci.*, 1992, **15**, 303–308.